

Preclinical evaluation and non-human primate receptor occupancy study of ^{18}F -JNJ-64413739, a novel PET radioligand for P2X7 receptors

Authors: Hartmuth C. Kolb¹, Olivier Barret², Anindya Bhattacharya¹, Gang Chen¹, Cristian Constantinescu², Chaofeng Huang¹, Michael Letavic¹, Gilles Tamagnan², Chunfang A. Xia¹, Wei Zhang¹, Anna Katrin Szardenings¹

¹*Janssen Research & Development LLC, 3210 Merryfield Row, San Diego, CA 92121, USA*

²*MNI, a division of inviCRO, 60 Temple Street, Suite 8A, New Haven, CT 06510, USA*

Corresponding Author: Anna Katrin Szardenings, Janssen Research & Development LLC, 3210 Merryfield Row, San Diego, CA 92121, USA. Phone: +1 858 320 3357. Email address: aszarden@its.jnj.com

First Author: Hartmuth C. Kolb, Janssen Research & Development LLC, 3210 Merryfield Row, San Diego, CA 92121, USA. Phone: +1 858 320-6942. Email address: hkolb1@its.jnj.com

Word Count: 4936

Running title: ^{18}F -JNJ-64413739 P2X7 PET tracer

Key words: P2X7 receptor, PET imaging, occupancy study

ABSTRACT

Background: The P2X7 receptor is an adenosine triphosphate (ATP)-gated ion-channel, which is abundantly expressed in glial cells within the central nervous system and in the periphery. P2X7 receptor activation leads to the release of the pro-inflammatory cytokine IL-1 β in the brain, and antagonism of the P2X7 receptor is a novel therapeutic strategy to dampen ATP-dependent IL-1 β signaling. PET ligands for the P2X7 receptor will be not only valuable to assess central target engagement of drug candidates, but also hold promise as surrogate markers of central neuroinflammation. Herein we describe the *in vitro* and *in vivo* evaluation of ^{18}F -JNJ-64413739, an ^{18}F -labelled PET ligand for imaging the P2X7 receptor in the brain.

Methods: P2X7 receptor affinity and specificity, pharmacokinetics, metabolic stability, blood-brain barrier permeability, and off-target binding of JNJ-64413739 were evaluated in a series of *in vitro*, *ex vivo*, and *in vivo* assays. ^{18}F -JNJ-64413739 was radio-labelled via a one-step nucleophilic aromatic substitution. The tracer was also studied in rhesus macaques and PET images were analyzed with an arterial plasma input function-based Logan graphical analysis (LGA).

Results: The potency (IC_{50}) of the P2X7 receptor antagonist JNJ-64413739 is 1.0 ± 0.2 nM and 2.0 ± 0.6 nM at the recombinant human and rat P2X7 receptor, respectively, and the binding affinity K_i is 2.7 nM (rat cortex binding assay) and 15.9 nM (human P2X7 receptor). In non-human primate PET imaging studies, dose-dependent receptor occupancy (RO) of JNJ-54175446 was observed in two rhesus monkeys. At a 0.1 mg/kg dose (i.v.) of JNJ-54175446, the RO was calculated to be 17% by LGA, while a dose of 2.5 mg/kg yielded a RO of 60%.

Conclusion: The preclinical evaluation of ^{18}F -JNJ-64413739 demonstrates that the tracer engages the P2X7 receptor. Reproducible and dose-dependent receptor occupancy studies with the P2X7 receptor

antagonist JNJ-54175446 were obtained in rhesus monkeys. This novel PET tracer exhibits *in vitro* and *in vivo* characteristics suitable for imaging the P2X7 receptor in the brain and warrants further studies in humans.

INTRUCTION

The P2X7 receptor belongs to the P2X family of trimeric ligand-gated cation channels, and its activation by ATP allows for the flux of several cations, including Ca^{2+} , Na^+ , and K^+ (1,2). The ATP-gated purinergic P2X7 receptor is abundantly expressed in CNS microglia (3). In the brain the P2X7 receptor is expressed ubiquitously as demonstrated by immunohistochemistry, autoradiography and PET imaging (4,5,6). At a functional level, the P2X7 receptor is activated by high concentrations of ATP. Under normal physiological conditions, extracellular ATP concentrations are generally below the threshold required for P2X7 receptor activation, and P2X7 receptor signaling is believed to be silent. However, during CNS pathology extracellular ATP levels can reach sufficiently high concentrations to activate the receptor, as has been demonstrated with P2X7 receptor antagonists in models of disease (7). Hence, while P2X7 receptor expression levels are detectable or high in normal CNS tissues, their ion channel activity might be low or inactive. While expression levels may or may not be upregulated during a neuroinflammatory response, the ion channel activity will most likely be engaged in a disease state making a case for targeting the P2X7 receptor as an attractive drug target for CNS therapeutics (8).

One of the features of the P2X7 receptor activation is NLRP3 inflammasome activation followed by release of pro-inflammatory cytokines IL-1 β and IL-18 (9), which is dependent on two critical steps working in concert: (a) a priming of toll-like receptors by LPS and (b) a subsequent activation of the P2X7 receptor by ATP, such that each one on its own will be unable to trigger P2X7 receptor mediated IL-1 β /IL-18 release. The release of these cytokines triggers a cascade of downstream events leading to microglial activation,

astrogliosis and ultimately neuroinflammation. Once the P2X7 receptor is activated, it also serves as a conduit for further intracellular ATP release (10), leading to a self-propelled increase of an inflammatory response. In animal models of neuroinflammation, such as ones induced by LPS, polyI:C, BCG, IFN- α , or kainic acid, it is critical to model the priming step and generate sufficient extracellular ATP to engage P2X7 receptor dependent IL-1 β release in the brain. This was elegantly demonstrated by Territo et al. (11), who used a high dose LPS (5 mg/kg) model of neuroinflammation to show enhanced brain uptake of ^{11}C -GSK1482160, a P2X7 receptor PET ligand. Likewise, in a model of multiple sclerosis, the same PET ligand was shown to have higher retention in the spinal cord (12), suggesting P2X7 receptor up-regulation in these extreme conditions in rodents. Due to the intricate link of P2X7 receptor activation with IL-1 β release and neuroinflammation, there is a lot of interest in developing clinical candidates that are both P2X7 receptor antagonists and PET ligands. While the former class of molecules may be useful to treat CNS disorders with a neuroinflammatory component, PET ligands for the P2X7 receptor may serve a dual purpose: (a) for use in the clinic as a biomarker to support central target engagement of the P2X7 receptor and (b) for use as tools to study neuroinflammation.

We have published several classes of brain penetrant P2X7 receptor antagonists, including our clinical compound JNJ-541754464. Our team has disclosed a ^{11}C -labeled P2X7 receptor PET ligand JNJ-54173717 (13), which was successfully used to detect basally overexpressed P2X7 receptors in rat brains. In these models, the PET signal was blocked by competition with cold P2X7 receptor ligands in a dose dependent manner. Similarly, the ^{11}C -GSK1482160 PET signal in the brain of LPS challenged rats was also blocked by a cold P2X7 antagonist, demonstrating specificity of the PET signal to P2X7 receptors. In addition to ^{11}C -JNJ-54173717 and ^{11}C -GSK1482160, two other groups have disclosed P2X7 receptor PET ligands (^{11}C -A-7400003, and ^{18}F -EFB), albeit with no data to support target specificity of these tracers (14,15). Most

recently, ¹¹C-SMW139, was described as a brain permeable and selective P2X7 receptor ligand by B. Janssen et al. with promising results obtained in a rat model overexpressing human P2X7 receptor (16)

Here, we report a new P2X7 receptor PET ligand, ¹⁸F-JNJ-64413739, to support our clinical therapeutic candidate, JNJ-54175446, with occupancy studies. In addition, this ligand will be used to study conditions of neuroinflammation. This manuscript describes the radiochemistry, preclinical pharmacology and non-human primate PET data in support of ¹⁸F-JNJ-64413739 as a best in class CNS penetrant P2X7 receptor PET ligand.

MATERIALS AND METHODS

Synthesis of precursor and standard are provided in Supplemental Data

Radiochemistry

The radiotracer used in this study is a sterile, non-pyrogenic solution of no-carrier-added ¹⁸F-JNJ-64413739 in a formulation solution. The radiotracer was prepared by reaction of the corresponding chloro precursor, (S)-(3-chloro-2-(trifluoromethyl)pyridin-4-yl)(6-methyl-1-(pyrimidin-2-yl)-6,7-dihydro-1H-[1,2,3]triazolo[4,5-c]pyridin-5(4H)-yl)methanone (JNJ-64410047), with fluorine-18 fluoride in the presence of potassium carbonate and Kryptofix-222 (Fig. 1) using a commercial synthesizer, GE TRACERlab® FX-FN.

Purification was performed by reverse phase HPLC using a Phenomenex Luna C18(2) column (10 µm, 10 x 250 mm) eluted with a mixture of acetonitrile/water/ trifluoroacetic acid (40/60/0.1, v/v/v) at a flow rate of 4 mL/min. The product fraction was collected in a flask containing 20 mL of diluted sodium ascorbic in water for injection (WFI). The diluted product mixture was passed through a solid-phase extraction cartridge (SPE, Sep-Pak® C18 Light) and the cartridge was rinsed with 10 mL of diluted sodium ascorbic in

WFI. The radiolabeled product was eluted from the SPE cartridge with 1.0 mL of 200-proof USP grade ethanol into the formulation flask, pre-loaded with 10 mL of formulation base (diluted sodium ascorbate containing PS-80). The Sep-Pak® cartridge was rinsed with 4 mL of formulation base and the rinse was mixed with the contents of the formulation flask. The resulting solution was passed through a sterilizing 0.2 µm membrane filter into a sterile, filter-vented final product vial.

Quality control testing included visual inspection of appearance. Identity, chemical, and radiochemical purity were determined by HPLC. Strength was measured by gamma assay. Filter integrity, pyrogen content, and sterility were determined by compendial tests per USP. Residual solvents were determined by GC. pH was measured using pH paper. A total of seven preparations with an average tracer purity of 99.8 ± 0.3 % were used during this study. The average decay corrected radiochemical yield was 3.1 ± 2.0 % and the average molar activity at the end of synthesis was 48.3 ± 22.3 GBq/µmol.

In Vitro Pharmacology – Ki, IC50 In Human and Rat

For in vitro functional assays 1321N cell lines expressing either the rat or human P2X7 receptor, the agonist 2(3)-O-(4-benzoylbenzoyl)adenosine 5-triphosphate (Bz-ATP) was used for channel activation, and JNJ-41857660 as the reference compound ($pIC_{50}=6.3 \pm 0.5$). Radioligand binding experiments were conducted using [³H]-A804598 and 1321N1 cells expressing the recombinant human and rat P2X7 receptor. Experimental details are provided in the supplemental section.

Microdosing Experiments in Rodents

Animals/rodents: Animal studies were conducted in the United States in accordance with the Guide for the Care and Use of Laboratory Animals (17). Studies performed in Europe were in accordance with the European Communities Council Directive 2010/63/EU (18) and local legislation on animal

experimentation. Facilities were accredited by the Association for the Assessment and Accreditation of Laboratory Animal Care. Animals were allowed to acclimate for 5 days after receipt. They were housed in accordance with institutional standards, received food and water ad libitum, and were maintained on a 12-hour light/dark cycle.

To evaluate the brain biodistribution of JNJ-64413739 in rodents at a microdose level, rats (n = 3 each group) were administered with a single intravenous dose of 0.03 mg/kg of JNJ-64413739 formulated in 20% (w/v) HP- β -Cyclodextrin in ddH₂O, pH7.4. A blocking experiment was performed by p.o. administration of the P2X7 antagonist JNJ-55308942 (19) (5 mg/kg) 1 hour before microdosing of JNJ-64413739. At two time points (15 and 30 minutes) following microdosing, the cerebrums were collected and homogenized to analyze JNJ-64413739 levels by LC-MS/MS.

P2X7 receptor knockout (KO) mice were used to measure non-specific binding of JNJ-64413739 (20). The KO strain was a mixed genetic background of 129/Ola_C57BL/6_DBA/2 and was obtained under a license from JAX (catalog # 005576). KO and strain matched wild type (WT) mice (n=4 each) were dosed intravenously with JNJ-64413739 (0.1mg/kg of body weight). Cerebrums were harvested after 30 min for LC-MS/MS analysis.

LC/MS/MS analysis: JNJ-64413739 brain homogenate samples were extracted using a protein precipitation method and analyzed on an API4000 Q-Trap MS/MS System (Applied Biosystems, Concord, Ontario, Canada) interfaced with a Shimadzu LC high-performance liquid chromatographer. Samples were loaded onto a 2.1 × 50-mm Gemini, NX-C18, 3 μ m 110A column (Phenomenex, Torrance, CA, US) under a flow rate of 0.5 ml/min using water (0.1% formic acid) as mobile phase A and acetonitrile (0.1% formic acid) as mobile phase B. Starting with 85% mobile phase A for 0.5 minutes, mobile phase B was increased from 15% to 98% using a linear gradient for 1.1 minute, held at 98% B for 0.6 minutes, and equilibrated

at 15% B for 0.4 minutes for an overall run time of 2.5 minutes. JNJ-64413739 was quantified by MS/MS in the positive ion mode by monitoring the transition of 408 to 172 m/z.

Non-human Primate Brain PET Imaging Studies (at MNI/Invicro)

Animals. All experiments were conducted in accordance with the United States Public Health Service's Policy on Humane Care and Use of Laboratory Animals and with institutional approval. Adult rhesus macaques (*Macaca mulatta*, 1 female and 1 male, 10.3 ± 2.3 kg) were used. An intravenous catheter was used for administration of fluids for hydration. Body temperature was maintained by a heated water blanket and monitored with a rectal thermometer. Vital signs were monitored continuously and recorded every 10–20 min during the study.

Vehicle and Blocking Agent. JNJ-54175446 was formulated in a vehicle of acetate buffer (100 mM, pH = 4.5) containing 20% of PEG400 and 20% of HP- β -CD. The concentration of the solution was determined by HPLC (Xbridge C18, methanol/ammonium acetate 5 mM, 70/30, 1 mL/min, 254 nm) by comparison with a 1 mg/mL standard solution in DMSO. Vehicle only or JNJ-54175446 at doses of 0.1, 0.4, 2.5 (duplicate) and 5.3 mg/kg were administered intravenously over 3 min, starting 10 min before tracer injection. Blood samples were taken at -5 (pre-dose), 10, 20, 40, 70, 100, and 130 min relative to the start of JNJ-54175446 injection to measure its plasma levels during PET imaging.

PET Acquisition. PET scans ($n = 7$) were performed on a Siemens Focus 220 microPET camera (Siemens Healthcare Molecular Imaging, Knoxville, TN, USA) following IV administration of 179.8 ± 9.9 MBq of ^{18}F -JNJ-64413739: two scans with vehicle only and 5 scans after blocking with JNJ-54175446. PET images were acquired over a period of 2 hours. The dynamic series was reconstructed using filtered back projection with corrections for random, scatter, and attenuation.

Arterial Input Function. Arterial blood samples were collected over 2 hours after tracer administration. Radioactivity in whole blood and plasma were measured in all samples. A subset of plasma samples was processed by acetonitrile denaturation, and radio-metabolites and parent fractions were measured by reverse-phase HPLC performed on a Phenomenex Luna C18(2) (10 x 250 mm, 10 μ m) column eluted with a mobile phase consisting of a mixture of methanol / water with 0.2% of triethylamine in a 65/35 ratio at a flow rate of 4 mL/min. Plasma radioactivity and parent fraction curves were used to generate the metabolite corrected arterial input function. The plasma protein binding free fraction (f_p) was measured by ultrafiltration (Centrifree[®], Millipore).

Image Processing. PET images were analyzed in PMOD 3.6 (PMOD Technologies, Zurich, Switzerland) and were motion corrected when necessary. The first post vehicle image of each primate was normalized to an MR rhesus brain template (21). Subsequent images of the same primate were co-registered to their corresponding vehicle image thus transforming each image to a standard space. A volume of interest (VOI) ATLAS template including multiple brain regions with variable tracer uptake was applied to the PET images, time activity curves (TAC) of the average activity concentration over time within each region were generated. TACs were expressed in Standardized Uptake Value (SUV) units (g/mL) by normalizing by the weight of the animal and the injected dose.

Kinetic Modeling and Analysis. All kinetic analyses were performed using PMOD 3.6. The plasma-based Logan graphical analysis (LGA) (22), with a cutoff t^* fixed at 20 min, was applied to the regional TACs using the arterial plasma input function corrected for radio-metabolites to determine the total volume of distribution V_T for each brain region (23). No region in the brain devoid of P2X7 receptor could be identified, and the occupancy at each JNJ-54175446 dose was estimated using the global occupancy plot (24), with $V_T^{\text{Baseline}} - V_T^{\text{JNJ446}}$ on the y-axis and V_T^{Baseline} on the x-axis, where V_T^{Baseline} is the V_T at baseline, and

V_T^{JNJ446} is the V_T following JNJ-54175446 administration. The occupancy is given by the slope of the linear regression, and the non-displaceable distribution volume, V_{ND} , is given by the x-intercept.

RESULTS

In Vitro Pharmacology

The potency (IC_{50}) of JNJ-64413739 is 1.0 ± 0.2 nM ($n=3$, recombinant human P2X7 receptor) and 2.0 ± 0.6 nM ($n=3$, recombinant rat P2X7 receptor), and the binding affinity K_i is 2.7 nM (1.7, 3.8) in a rat cortex binding assay and 15.9 nM (14, 18) for the human P2X7 receptor. In-vitro microsomal stability testing suggested excellent metabolic stability in humans ($T_{1/2} = 180$ minutes) and rats ($T_{1/2} >60$ minutes). Human plasma protein binding was determined to be 63% (free fraction) and the free fraction in rat brain tissue was 19%, which are in an acceptable range for a PET ligand (25).

Pharmacokinetics and Metabolism in Rats

Absorption and Pharmacokinetics

An MDR1-MDCK permeability assay (P-glycoprotein substrate identification) was performed to assess CNS permeability of the compound and to characterize whether it is a P-gp substrate. The efflux ratio was determined to be 13.8. To determine the pharmacokinetic profile of this antagonist, a single i.v. dose of JNJ-64413739 at 1 mg/kg was administered to male SD rats ($n=3$). Plasma levels were determined at different time-points for 4 hours post-dosing (Fig. 2).

A maximum plasma concentration of 1107 ng/mL was reached at 2 minutes post-injection. The AUC_{∞} was determined to be 459 h.ng/mL with a CL of 36.6 mL/min/kg (Table 3).

The blood brain barrier permeability of JNJ-64413739 was assessed by administering the compound IV at 1 mg/kg to male SD rats. The concentrations of JNJ-64413739 in plasma and brain homogenate were measured at different time points post-dosing (Fig. 3). The brain/plasma ratio was 0.8 at 5 minutes, 0.91 at 30 minutes, 0.92 at 60 minutes, and 1.08 at 120 minutes post-injection, respectively.

Microdosing Experiments

For microdosing/blocking experiments with JNJ-64413739 (0.03 mg/kg, i.v. dosing) in rats, all animals (n=3 per group) were pretreated p.o. with the P2X7 antagonist JNJ-55308942 (5 mg/kg or vehicle) 1 hour before administration of JNJ-64413739. Brain uptake of JNJ-64413739 in the pretreatment group decreased by 42.3% (15 min) and 43.7% (30 min) compared with the control group (vehicle only, n=3) (Fig. 4). In a microdosing experiment with JNJ-64413739 (0.1 mg/kg, i.v. dosing) in wild-type and P2X7 receptor KO mice, compound levels in the brains of KO mice (n=4) after 30 minutes were 38% lower than that in WT mice (Fig. 5).

PET imaging in Rhesus Monkeys

In vivo PET studies in rhesus macaque monkeys confirmed rapid brain uptake peaking within 10 minutes (up to 1.5 to 2 SUV in cortical and subcortical regions, and cerebellar cortex), slowly clearing from the brain over the next 2 hours (Fig. 6). The diffuse distribution of the signal in the brain was consistent with the known wide-spread distribution of the P2X7 receptor on astrocytes and microglia, which also precluded identification of a reference region for modeling and quantifying the tracer uptake using brain tissue activity alone. The volume of distribution of the signal V_T could be readily estimated from graphical analysis of the tissue curves using the arterial input function and arterial sampling is planned in the initial studies in humans.

^{18}F -JNJ-64413739 was stable in blood *ex vivo* and showed good metabolic stability *in vivo* with 40% and 20% of parent tracer remaining at 30 and 120 min post injection, respectively, with a high protein-binding free fraction in plasma of $72.3\% \pm 2.5\%$ ($n=7$). ^{18}F -JNJ-64413739 metabolism was not altered by the presence of JNJ-54175446. Signal accumulation in bone was not observed (no defluorination), suggesting this will not confound quantitation of the ^{18}F -JNJ-64413739 brain signal. ^{18}F -JNJ-64413739 V_T values computed with LGA post vehicle ranged from ~ 1.7 in the cerebellar cortex to ~ 2.4 - 2.7 in the thalamus. The global brain distribution of ^{18}F -JNJ-64413739 was reduced in a dose dependent manner by pretreatment with 0.1 ($\sim 18\%$ occupancy) to 5 mg/kg ($> 50\%$ occupancy) JNJ-54175446 i.v. in rhesus monkey (Table 4). Dose dependency of ^{18}F -JNJ-64413739 binding to the P2X7 receptor is demonstrated in Fig. 5 by comparing the TACs acquired in the vehicle study to the JNJ-54175446 pretreatment studies at different doses.

Occupancy estimates for both monkeys reached a plateau at around $\sim 55\%$. At highest doses, V_T was reduced and ranged from ~ 1.5 in the cerebellar cortex to ~ 1.8 in the thalamus, while from the occupancy plots, the non-displaceable volume of distribution V_{ND} was estimated to 1.2 ± 0.1 . This indicates a certain level of non-specific binding of ^{18}F -JNJ-64413739.

DISCUSSION

The study characterizes a novel ^{18}F -fluorinated P2X7 receptor antagonist PET ligand, JNJ-64413739. P2X7 receptors are abundantly expressed in brain microglia and are a potential drug target for neuroinflammatory disorders. The Janssen team has recently disclosed two clinical candidates, JNJ-54175446 (4) and JNJ-55308942 (18), both of which are CNS penetrant P2X7 receptor antagonists. In CNS drug development, unequivocal demonstration of central target engagement in both human subjects (phase-1) and patients (phase-2) are critical in dose selection during pivotal proof-of-concept studies. The

preclinical studies described here in detail demonstrate that ¹⁸F-JNJ-64413739 is a PET ligand that binds to the P2X7 receptor at the same site as JNJ-54175446 and JNJ-55308942 and will be a critical tool in demonstrating human brain binding of our P2X7 receptor clinical compounds.

JNJ-64413739 is a potent (IC₅₀ 1 nM, K_i 16 nM human P2X7 receptor) antagonist. Brain uptake and selectivity of the cold compound were assessed by MS/MS analysis of brain tissues in rats in blocking experiments and in a KO mouse model. Brain/plasma ratios in rats are close to 1 and brain uptake is moderate. Microdosing blocking experiments and residual binding in the KO mouse model suggest a certain degree of non-specific binding of this tracer in brain tissue. However, since the animals used in these experiments had no neuroinflammatory pathology, baseline levels/activity of the target can also be expected to be generally low. The evaluation of ¹⁸F-JNJ-64413739 in neuroinflammatory models will be reported in due course elsewhere. Occupancy studies in rhesus monkeys reached a plateau at 55-60% at the highest doses, which agrees with the findings in rodents. However, the PET signal was blocked in a dose-dependent manner and the tracer showed excellent metabolic stability with little protein binding. No bone uptake was observed. The findings encourage us to move forward with ¹⁸F-JNJ-64413739 to measure occupancies of the therapeutic JNJ-54175446 in the clinic.

PET displacement data shown in monkeys usually mirror closely human data, providing confidence that data obtained from monkey brain using PET imaging can be used with high degree of translational validity. In addition to using ¹⁸F-JNJ-64413739 as a clinical imaging agent to aid in P2X7 receptor drug development efforts, P2X7 receptor PET ligands may also offer new hope in probing CNS microglial activation. TSPO remains the only marker of microglial activation so far and there have been numerous reports and reviews of TSPO PET ligands (26). P2X7 receptor PET imaging may offer a unique opportunity to compare TSPO PET signals from patients suffering from neurodegeneration and neuropsychiatric illnesses. Based on the role of P2X7 receptors in neuroinflammation, there is hope that P2X7 receptor PET may complement, if

not replace, TSPO PET ligands, which have shown limitations in the clinic due to polymorphism and high signal-to-noise ratios (27). P2X7 receptor upregulation in neuroinflammation is subtle and thereby high affinity PET ligands may be useful for patient stratification.

CONCLUSION

In conclusion, ¹⁸F-JNJ-64413739 behaves as a suitable PET ligand for the P2X7 receptor and has shown dose dependent competitive binding with JNJ-54175446 in monkey PET studies, in vivo. It therefore could be a useful PET ligand for receptor occupancy studies in human.

FIGURES

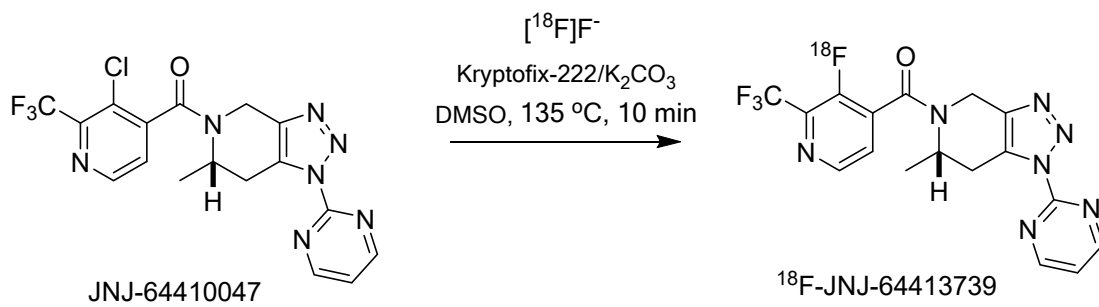


FIGURE 1: Radiosynthesis of ^{18}F -JNJ-64413739

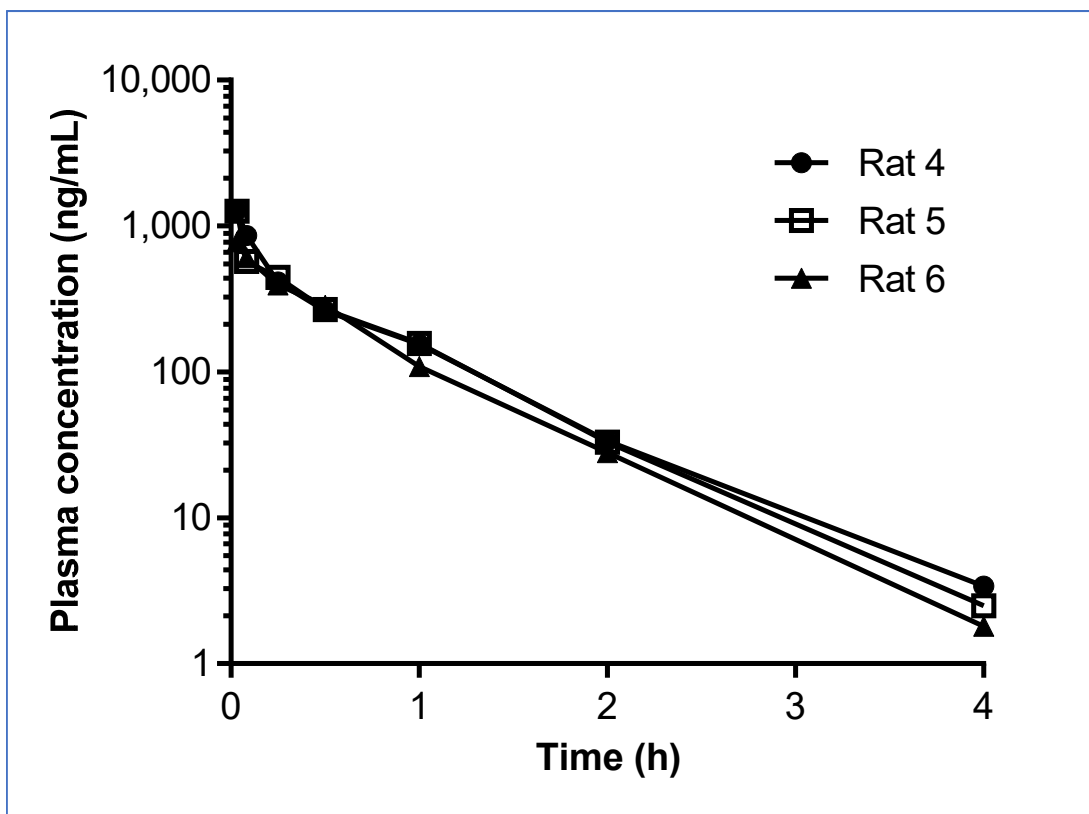


FIGURE 2: Rat i.v. pharmacokinetics profile: time vs plasma concentration of JNJ-64413739 (n=3)

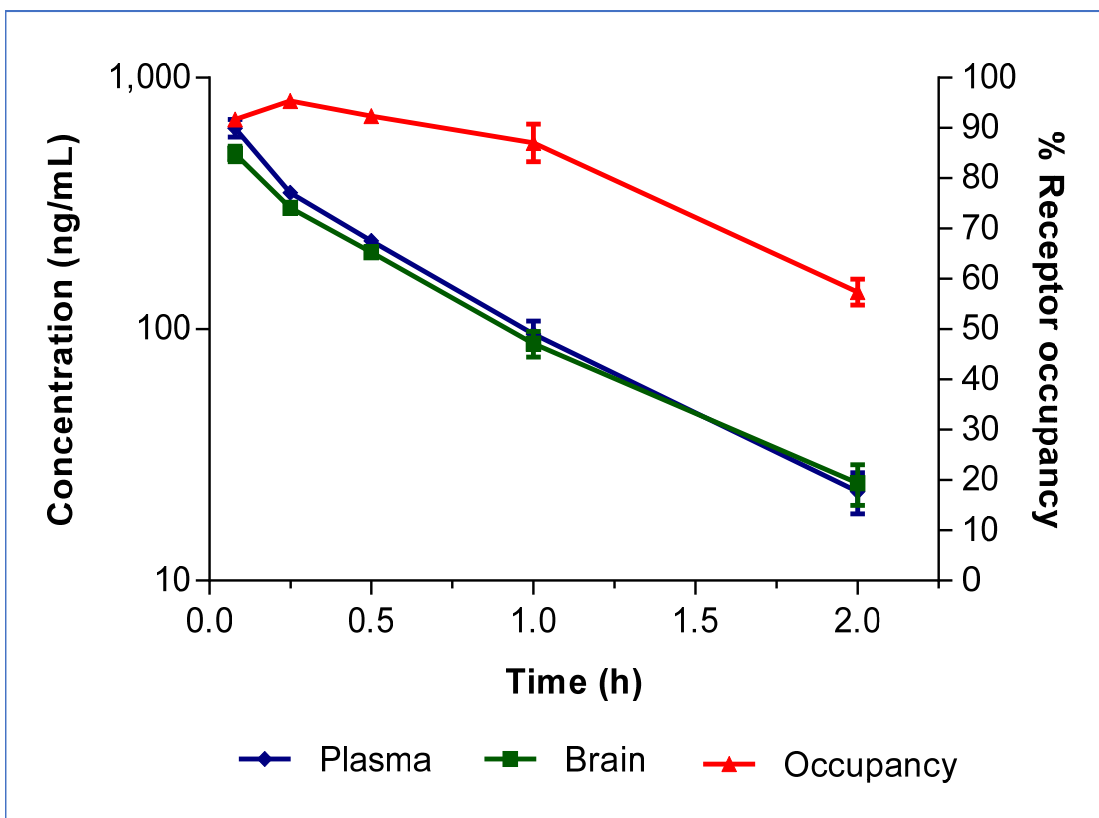


FIGURE 3: Brain vs plasma concentration of JNJ-64413739 in rats (n=3) over time

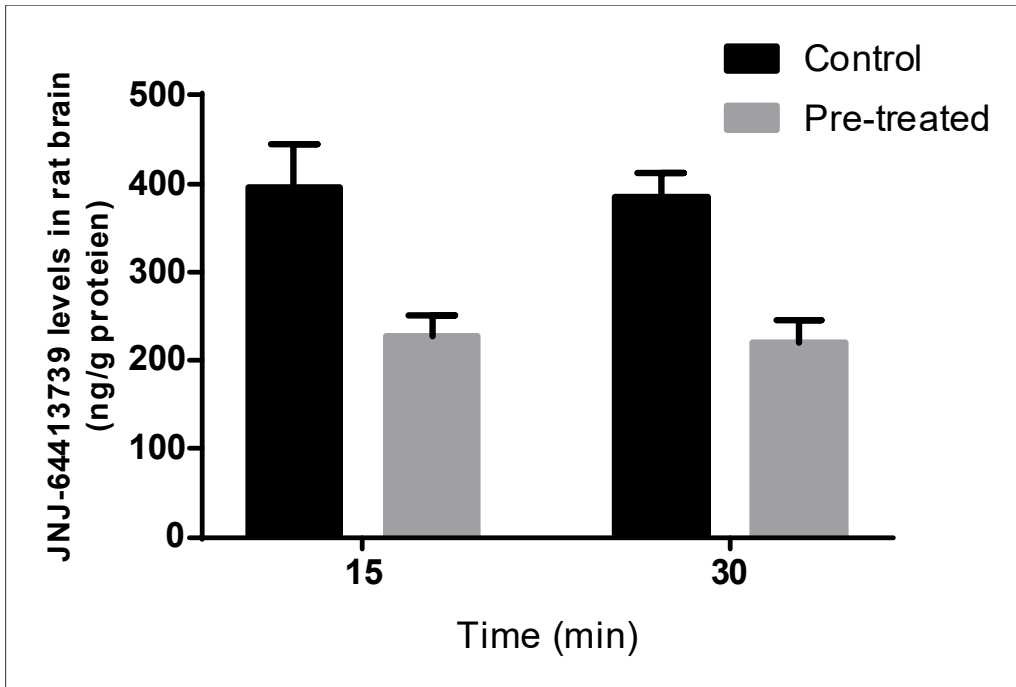


FIGURE 4: Microdosing blocking of retention of JNJ-64413739 in rat brain pretreated with JNJ-55308942 or vehicle (n=3, each). *P<0.01 vs. control

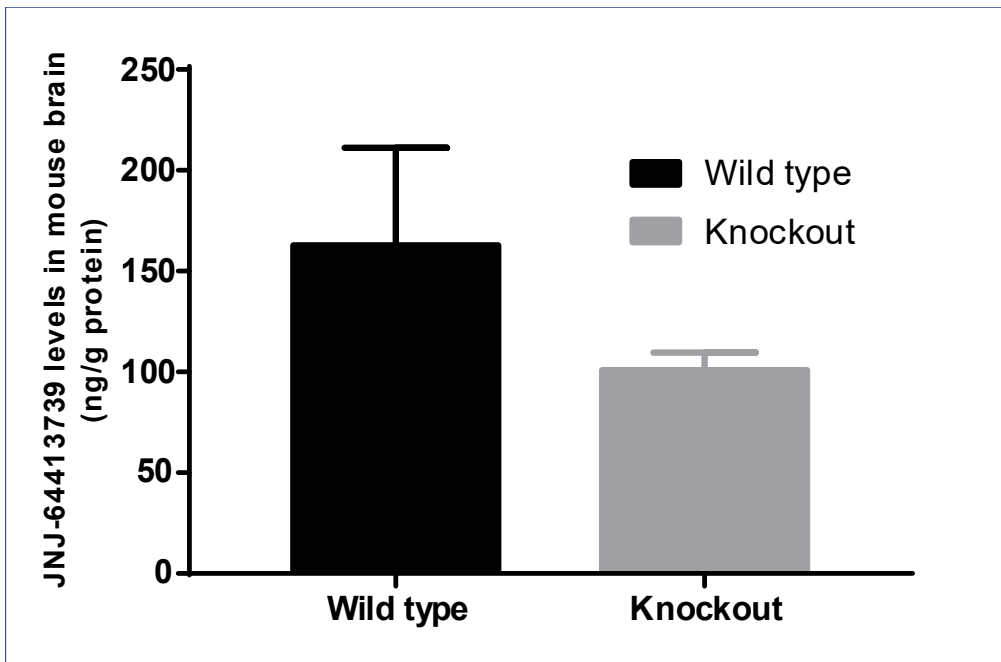


FIGURE 5: Brain uptake/retention of JNJ-64413739 in wild type and knockout mice (n=4, each). *P<0.05 vs. wild type.

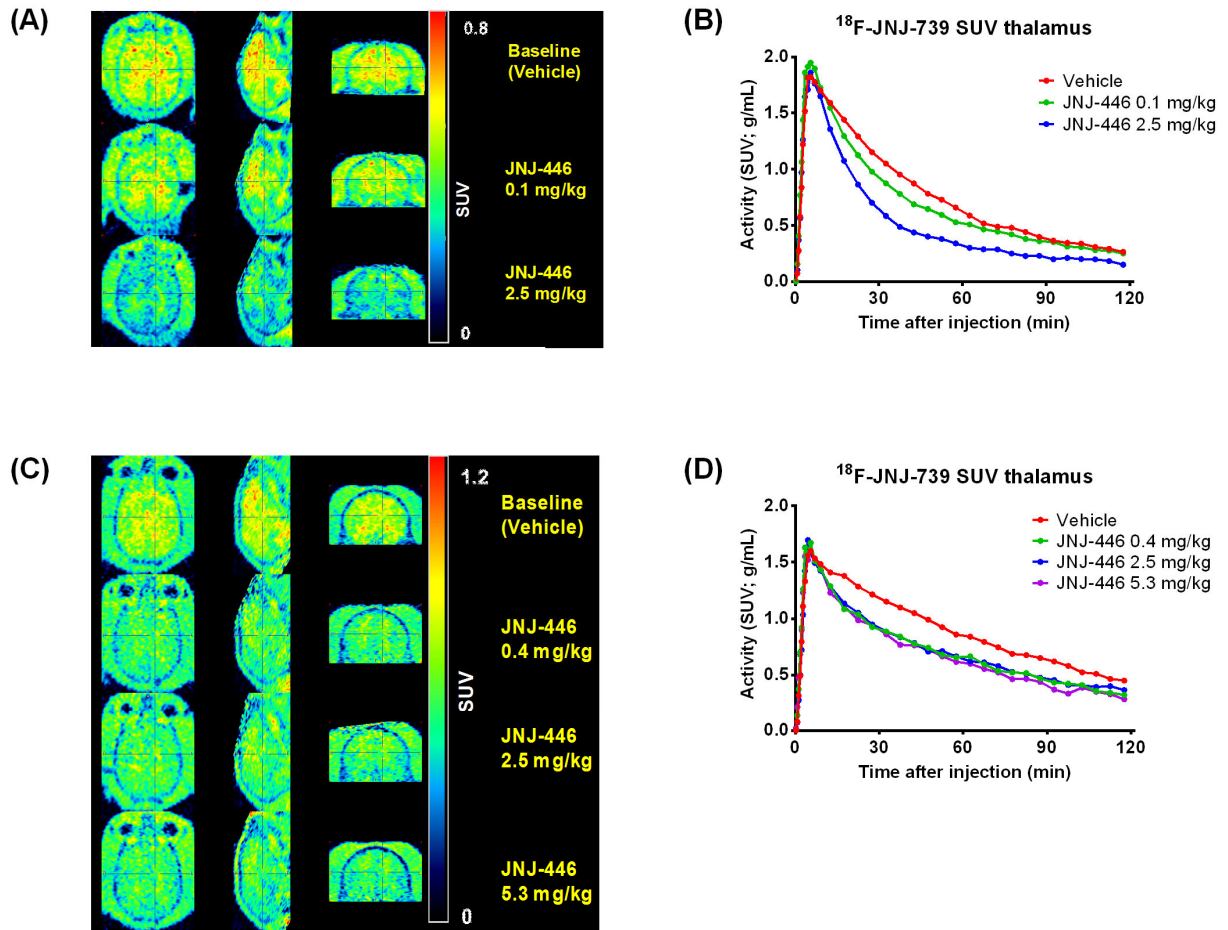


FIGURE 6: ^{18}F -JNJ-64413739 NHP PET: Blocking with a P2X7 inhibitor JNJ-54175446. Summed images 30-120 min normalized to SUV acquired following either vehicle or JNJ-54175446 at different dose levels are shown for (A) monkey 1 and (C) monkey 2. Corresponding time-activity curves of the thalamus expressed as SUV are shown for (B) monkey 1 and (D) monkey 2. Key: JNJ-739 = JNJ-64413739, JNJ-446 = JNJ-54175446.

TABLES

Assay	JNJ-64413739
IC ₅₀ P2X7 human (nM)	1.0 ± 0.2
IC ₅₀ P2X7 rat (nM)	2.0 ± 0.6
Ki P2X7 human (nM)	15.9 ± 2.0
Ki P2X7 rat (nM)	2.7 ± 1.1

TABLE 1: IC₅₀ and Ki values for JNJ-64413739 (mean ± SD)

Rat	CL	CL	V _d	V _{ss}	AUC _{INF}	C ₀	C ₀	T1/2 _{terminal}
ID	(ml/min/kg)	(L/kg)	(L/kg)	(L/kg)	(hr*ng/mL)	(ng/ml)	(μM)	(hr)
4	33.6	2.0	1.6	1.3	497	1660	4.1	0.6
5	34.8	2.1	1.5	1.3	479	2119	5.2	0.5
6	41.6	2.5	1.8	1.6	401	921	2.3	0.5
Mean	36.6	2.2	1.7	1.4	459	1567	3.8	0.5
SD	4.3	0.3	0.2	0.1	51	604	1.5	0.0
CV%	12	12	9	11	11	39	39	5

TABLE 2: Rat i.v. pharmacokinetics parameters of JNJ-64413739

Dose (mg/kg)	AUC (ng/mL*min)	%RO	Monkey
5.3	132470	51.7	2
2.5	46991	60.4	1
2.5	42353	55.1	2
0.4	5764	52.1	2
0.1	2102	17.6	1

TABLE 3: Target occupancy of JNJ-54175446 in non-human primates

ACKNOWLEDGEMENTS

We would like to thank Brian Lord for generating pharmacokinetics and occupancy data in rats, Hong Ao for IC50 and Ki determination, and Leslie Nguyen for PK analysis of the microdosing samples.

DISCLOSURES

A. Bhattacharya, G. Chen, C. Huang, H. Kolb, M. Letavic, K. Szardenings, C. Xia, and W. Zhang are employed by Janssen, who provided financial support for this research project. O. Barret, C. Constantinescu, and G. Tamagnan were employed by MNI, Molecular Neuroimaging, LLC, now inviCRO, who were contracted by Janssen to perform the non-human primate studies. No other potential conflicts of interest relevant to this article exist.

REFERENCES

- ¹ Bartlett R, Stokes L, Sluyter R. The P2X7 receptor channel: recent developments and the use of p2x7 antagonists in models of disease. *Pharmacol Rev.* 2014;66:638-675.
- ² Sperlagh B, Illes P. P2X7 receptor: an emerging target in central nervous system diseases. *Trends in Pharmacol Sci.* 2014;35:537-547.
- ³ Bhattacharya A, Biber K. The microglial ATP-gated ion channel P2X7 as a CNS drug target. *Glia.* 2016;64:1772-1787.
- ⁴ Letavic MA, Savall BM, Allison BD, et al. 4-Methyl-6,7-dihydro-4H-triazolo[4,5-c]pyridine-based P2X7 receptor antagonists: optimization of pharmacokinetic properties leading to the identification of a clinical candidate. *J Med Chem.* 2017;60:4559-4572.
- ⁵ Lord B, Ameriks MK, Wang Q, et al. A novel radioligand for the ATP-gated ion channel P2X7: [³H] JNJ-54232334. *Eur J Pharmacol.* 2015;765:551-559.
- ⁶ Ory D, Celen S, Gijsbers R, et al. Preclinical evaluation of a P2X7 receptor-selective radiotracer: PET studies in a rat model with local overexpression of the human P2X7 receptor and in nonhuman primates. *J Nucl Med.* 2016;57:1436-1441.
- ⁷ Chrovian CC, Rech JC, Bhattacharya A, et al. P2X7 antagonists as potential therapeutic agents for the treatment of CNS disorders. *Pro Med Chem.* 2014;53:65-100.
- ⁸ Rech JC, Bhattacharya A, Letavic MA, et al. The evolution of P2X7 antagonists with a focus on CNS indications. *Bioorganic Med. Chem. Lett.* 2016;26:3838-3845

-
- ⁹ He Y, Taylor N, Fourgeaud L, Bhattacharya A. The role of microglial P2X7: modulation of cell death and cytokine release. *J Neuroinflammation*. 2017;14:135-147.
- ¹⁰ Cisneros-Mejorado A, Perez-Samartin A, Gottlieb M, et al. ATP signaling in brain: release, excitotoxicity and potential therapeutic targets. *Cell Mol Neurobiol*. 2015;35:1-6.
- ¹¹ Territo PR, Meyer JA, Peters JS, et al. Characterization of [¹¹C]-GSK1482160 for targeting the P2X7 receptor as a biomarker for neuroinflammation. *J Nucl Med*. 2017;58:458-465
- ¹² Han J, Liu H, Liu C, et al. Pharmacologic characterizations of a P2X7 receptor-specific radioligand, [¹¹C]GSK1482160 for neuroinflammatory response. *Nucl. Med. Commun*. 2017;38:372-382.
- ¹³ Ory D, Celen S, Gijbbers R, et al. Preclinical evaluation of a P2X7 receptor-selective radiotracer: PET studies in a rat model with local overexpression of the human P2X7 receptor and in nonhuman primates. *J Nucl Med*. 2016;57:1436-1441.
- ¹⁴ Fantoni ER, Dal Ben D, Falzoni S, et al. Design, synthesis and evaluation in an LPS rodent model of neuroinflammation of a novel 18F-labelled PET tracer targeting P2X7. *EJNMMI Res*. 2017;7:31-42.
- ¹⁵ Janssen B, Vugts DJ, Funke U, et al. Synthesis and initial preclinical evaluation of the P2X7 receptor antagonist [(¹¹C)A-740003 as a novel tracer of neuroinflammation. *J Labelled Comp Radiopharm*. 2014;57:509-516.
- ¹⁶ Janssen B, Vugts DJ, Wilkinson SM, et al. Identification of the allosteric P2X7 receptor antagonist [¹¹C]SMW139 as a PET tracer of microglial activation. *Sci Rep*. 2018; 8:6580

¹⁷ National Research Council: *Guide for the Care and Use of Laboratory Animals*, 8th ed, The National Academies Press, Washington, DC. 2011

¹⁸ European Union: *Directive 2010/63/EU of the European parliament and of the council of 22 September 2010 on the protection of animals used for scientific purposes*. Official Journal of the European Union: L 276:33–79

¹⁹ Chrovian CC, Soyode-Johnson A, Peterson AA, et al. A dipolar cycloaddition reaction to access 6-methyl-4,5,6,7-tetrahydro-1H-[1,2,3]triazolo[4,5-c]pyridines enables the discovery synthesis and preclinical profiling of a P2X7 antagonist clinical candidate. *J Med Chem*. 2018;61:207-223.

²⁰ Labasi JM, Petrushova N, Donovan C, et al. *J. Immunol*. 2002;168:6436-6445

²¹ Rohlfing CD, Kroenke EV, Sullivan MF, et al. The INIA19 Template and NeuroMaps Atlas for Primate Brain Image Parcellation and Spatial Normalization. *Front Neuroinform*. 2012;6:6-27

²² Logan J. A review of graphical methods for tracer studies and strategies to reduce bias. *Nucl Med Biol*. 2003;30:833-844

²³ Innis RB, Cunningham VJ, Delforge J, et al. Consensus nomenclature for in vivo imaging of reversibly binding radioligands. *J Cereb Blood Flow Metab*. 2007;27:1533-1539.

²⁴ Cunningham VJ, Rabiner EA, Slifstein M, et al. Measuring drug occupancy in the absence of a reference region: the Lassen plot re-visited. *J Cereb Blood Flow Metab*. 2010;30:46-50

²⁵ Zhang L, Villalobos A, Beck EM, et al. Design and Selection Parameters to Accelerate the Discovery of Novel Central Nervous System Positron Emission Tomography (PET) Ligands and Their Application in the Development of a Novel Phosphodiesterase 2A PET Ligand. *J Med Chem.* 2013;56:4568–4579

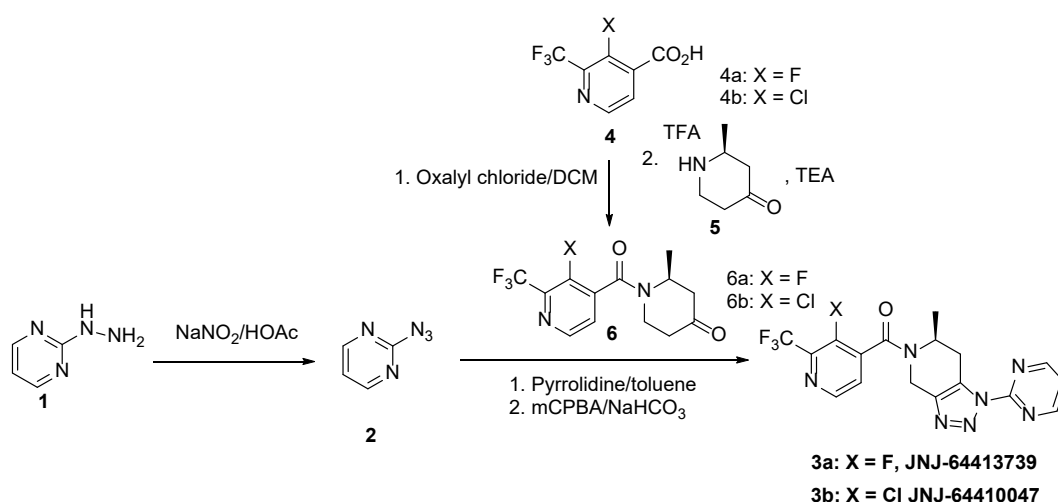
²⁶ Alam MM, Lee J, Lee SY. Recent progress in the development of TSPO PET ligands for neuroinflammation imaging in neurological diseases. *Nucl Med Mol Imaging.* 2017;51:283-296

²⁷ Vivash L, O'Brien TJ. Imaging microglial activation with TSPO PET: lighting up neurologic diseases? *J Nucl Med* 2016;57:165-8

Preclinical evaluation and non-human primate receptor occupancy study of ¹⁸F-JNJ-64413739, a novel PET radioligand for P2X7 receptors

SUPPLEMENTAL DATA

Synthesis of standard JNJ-64413739 and labeling precursor JNJ-64410047



Compounds 1, 4, and 5 were purchased from Anichem LLC (NJ, USA); ACES Pharma (NJ, USA) and Milestone Pharmtech USA Inc. (NJ, USA); all other reagents and solvents were purchased from commercial sources including Sigma-Aldrich (MO, USA), Thermo Fisher scientific (NH, USA), and VWR International (PA, USA).

Synthesis: Compounds 2, 3a/b and 6a/b were prepared according to a published procedure (18).

(S)-(3-fluoro-2-(trifluoromethyl)pyridin-4-yl)(6-methyl-1-(pyrimidin-2-yl)-6,7-dihydro-1H-[1,2,3]triazolo[4,5-c]pyridin-5(4H)-yl)methanone (**3a**, JNJ-64413739)

3a was prepared from compound **2** and **6a**. Yield 31% (using compound **6a** as the limiting reagent). MS (ESI): mass calcd. for C₁₇H₁₃F₄N₇O, 407.11; m/z found, 408.2 [M+H]⁺. ¹H NMR (500 MHz, Chloroform-*d*) δ

8.95-8.91 (m, 2H), 8.68-8.64 (m, 1H), 7.60-7.56 (m, 1H), 7.49-7.44 (m, 1H), 5.82, 5.65-5.62 (m, 1H), 4.69, 4.19-4.16 (m, 1H), 4.58-4.40 (m, 1H), 3.58-3.37 (m, 2H), 1.42-1.28 (m, 3H).

(S)-(3-chloro-2-(trifluoromethyl)pyridin-4-yl)(6-methyl-1-(pyrimidin-2-yl)-6,7-dihydro-1H-[1,2,3]triazolo[4,5-c]pyridin-5(4H)-yl)methanone (**3b**, JNJ-64410047)

3b was prepared from compound **2** and **6b**. Yield 40% (using compound **6b** as the limiting agent). MS (ESI): mass calcd. for C₁₇H₁₃ClF₃N₇O, 423.08; m/z found, 424.1 [M+H]⁺. ¹H NMR (500 MHz, Chloroform-*d*) δ 8.84-8.79 (m, 2H), 8.65-8.57 (m, 1H), 7.37-7.31 (m, 2H), 5.79-5.72, 5.55 (m, 1H), 4.57, 3.97-3.93 (m, 1H), 4.38-4.30 (m, 1H), 3.44-3.16 (m, 2H), 1.32-1.29, 1.18-1.16 (m, 3H).

(S)-1-(3-fluoro-2-(trifluoromethyl)isonicotinoyl)-2-methylpiperidin-4-one (**6a**)

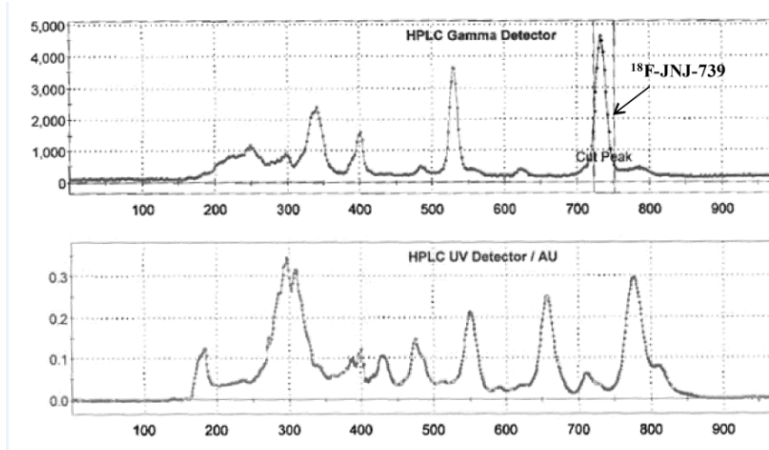
6a was prepared from compound **4a** and **5**. Yield 71%. MS (ESI): mass calcd. for C₁₃H₁₂F₄N₂O₂, 304.24 m/z found, 305.1 [M+H]⁺. ¹H NMR (500 MHz, Chloroform-*d*) δ 8.64-8.63 (m, 1H), 7.62-7.59 (m, 1H), 5.36-5.34, 3.36-3.31 (m, 1H), 5.02-4.98, 4.11-4.08 (m, 1H), 3.64 (m, 1H), 2.86-2.31 (m, 4H), 1.59-1.36 (m, 3H).

(S)-1-(3-chloro-2-(trifluoromethyl)isonicotinoyl)-2-methylpiperidin-4-one (**6b**)

6a was prepared from compound **4a** and **5**. Yield 59%. MS (ESI): mass calcd. for C₁₃H₁₂ClF₃N₂O₂, 320.05; m/z found, 321.1 [M+H]⁺. ¹H NMR (500 MHz, Chloroform-*d*) δ 8.62-8.60 (m, 1H), 7.44-7.19 (m, 1H), 5.33-5.25, 3.61-3.57 (m, 1H), 4.99-4.92, 3.92-3.90 (m, 1H), 3.47-3.22 (m, 1H), 2.79-2.72 (m, 1H), 2.61-2.24 (m, 3H), 1.31-1.26, 1.16-1.15 (m, 3H).

Radiochemistry

A representative HPLC trace for ¹⁸F-JNJ-64413739 is shown below (Supplemental Fig. 1).



SUPPLEMENTAL FIGURE 1: ¹⁸F-JNJ-64413739 representative HPLC trace

In Vitro Pharmacology – Ki, IC50 In Human and Rat

IC50 determination: 1321N1 cells expressing P2X7 receptor orthologs were dissociated 18–24 hours prior to the assay using 0.05% trypsin/EDTA (Invitrogen, Carlsbad, CA), and plated at density of 25,000 cells/well into poly-D-lysine-coated, 96-well, black-walled, clear-bottom plates (Becton-Dickinson, Bedford, MA). On the day of the experiment, cell plates were washed with assay buffer, containing the following: 130 mM NaCl, 2 mM KCl, 1 mM CaCl₂, 1 mM MgCl₂, 10mMHEPES, and 5 mM glucose at pH 7.40. After the wash, dye loading was achieved by adding a 2 Calcium-4 (Molecular Devices, Sunnyvale, CA) dye solution to the assay buffer. Cells were stained with the Calcium-4 dye in staining buffer for 30 minutes at room temperature in the dark. Test compounds were prepared at 250x of the final test concentration in neat dimethylsulfoxide. Intermediate 96-well compound plates were pre-pared by transferring 1.2 ml of the compound into 300 ml of assay buffer. A further 3x dilution occurred when transferring 50 ml/well of the compound plate to 100 ml/well in the cell plate. Cells were incubated with test compounds and dye for 30 minutes. Calcium flux was monitored in a Fluorometric Imaging Plate ReaderTetra as the cells

were challenged by adding 50 ml/well of Bz-ATP [29(39)-O-(4-benzoylbenzoyl) adenosine-59-triphosphate tri(triethylammonium)]. The final concentration of Bz-ATP was 250 mM.

Ki determination: ^3H -A-804598 (N-cyano-N99-[(1S)-1-phenylethyl]-N9-5-quinolinyl-guanidine) was used as the radioligand. P2 membranes were prepared from recombinant cells; 50 mM Tris-HCl (pH 7.4) was added to the cells and homogenized for approximately 30 seconds at high speed. The homogenate was centrifuged at 1500 rpm for 5 minutes followed by careful decanting of the supernatant, which was centrifuged at 32,000g for 30 minutes. Six milliliters of ice-cold assay buffer (50 mM Tris-HCl 1 0.1% bovine serum albumin) was added to the cell pellet. The reaction was incubated for 1 hour at 4°C. The assay was terminated by filtration (GF/B filters presoaked with 0.3% polyethylenimine) and washed with washing buffer (Tris-HCl 50 mM) repeatedly. After drying, the plate Microscint 0 was added to the filters and radioactivity was counted.

Liver Microsome Assay

The liver microsome assay was performed at Cyprotex (Watertown, MA, USA).

Test compounds are incubated over a time course to measure the half life ($t_{1/2}$), from which the following parameters are derived: the in vitro intrinsic clearance (Cl_{int}), the hepatic intrinsic clearance ($Cl_{int, H}$), the estimated in vivo hepatic clearance (Cl_H), and the extraction ratio (ER) using the simplified well-stirred model. It should be noted that in the simplified well-stirred model the values remain uncorrected for binding to both plasma and microsomal proteins (f_u^p and f_u^{mic}), and the blood to plasma ratio is assumed to be 1.

The test compound is incubated at a defined substrate concentration (typically 1 μM) in liver microsomes across a time course (typically 0, 5, 10, 20, 40, and 60 minutes). The reaction is terminated

by addition of a suitable organic solvent (typically, acetonitrile, methanol or DMSO). The samples are centrifuged prior to analysis by LC-MS/MS analysis. The relative amount of parent compound remaining in the active incubations vs. the control incubations (t=0 mins) for each compound is measured by peak area comparison.

Typical incubation conditions are: 1 μ M test compound, 0.5 mg/ml microsomal protein, 1 mM NADPH, 1 mM MgCl₂, and 0.1 M phosphate buffer, pH 7.4. Incubation volume is typically 500 μ L with a final total solvent of 0.01% DMSO and 0.5% acetonitrile.

1. Stock solutions of test compounds (typically 10 mM) are prepared in DMSO and further diluted into a 50:50 solution of acetonitrile:water to a working stock of 0.1 mM.
2. Liver microsomes are thawed and diluted to 0.5 mg/mL in 0.1 M phosphate buffer containing 1 mM MgCl₂. The diluted microsomes may be kept on ice and used within 30 min after thawing. NADPH stock solution is prepared and stored on ice.
3. A bulk liver microsomal mixture is prepared by spiking working stock of test compound (e.g. 5 μ L test compound + 395 μ L microsomal mixture), followed by thorough mixing.
4. The incubation plate containing the microsomal mixture is situated on a heater shaker unit located on the robot deck and is pre-incubated to 37°C (typically < 5 minutes).
5. The reaction is initiated by the addition of pre-warmed NADPH solution (typically 100 μ L).
6. Sequential aliquots are removed across a time course (typically 50 μ L) of the microsomal mixture are removed to a separate plate and quenched with acetonitrile (typically 200 μ L, which contains a genetic internal standard). Typically, the time points used are 0, 5, 10, 20, 40, and 60 minutes.
7. The plates are centrifuged (10 min at 4000 rpm in a cooled centrifuge) prior to analysis of the supernatant by LC-MS/MS.

- Typically, generic HPLC–MS/MS conditions are used for sample analysis in which specific SRM transitions are monitored for each compound. These transitions are usually optimized via automated procedures which are specific to the MS instrumentation used.

The percentage test compound remaining is calculated as the analytical response of test compound in the active sample divided by the average response of test compound in the control (t=0 min) samples. This result is expressed as a percentage, where the MS signal observed for test compound at t = 0 min is set to 100 % test compound remaining.

The *in vitro* metabolic half-life ($t_{1/2}$) is calculated using the slope of the log-linear regression from the percentage parent compound remaining versus time relationship (κ),

$$t_{1/2} = -\ln(2) / \kappa.$$

The *in vitro* intrinsic clearance (Cl_{int}) (ml/min/mg microsomal protein) is calculated using the following formula:

$$Cl_{int} = \frac{0.693}{t_{1/2}} \times \frac{V_{inc}}{W_{mic\ prot,inc}}$$

Where: V_{inc} = incubation volume, $W_{mic\ prot,inc}$ = weight of microsomal protein in the incubation

The hepatic intrinsic clearance ($Cl_{int,H}$) (ml/min/kg) is calculated using the following formula:

$$Cl_{int,H} = Cl_{int} \times MPPGL \times \frac{W_{liver}}{W_{body}}$$

Where MPPGL is the microsomal protein per gram liver i.e. W_{body} = body weight, W_{liver} = liver weight

The estimated *in vivo* hepatic clearance (Cl_H) (ml/min/kg) may be estimated using the equation for the Well Stirred Model

$$Cl_{H,blood} = \frac{Q_H \times \left(\frac{Cl_{int,H}}{f u_{mic}} \times \frac{f u_p}{B/P} \right)}{Q_H + \left(\frac{Cl_{int,H}}{f u_{mic}} \times \frac{f u_p}{B/P} \right)}$$

Where: Q_H = hepatic blood flow, $f u_p$ = the unbound fraction in plasma, $f u_{mic}$ = the unbound fraction in microsomes, and B/P = blood to plasma ratio

The extraction ratio (ER) is determined as follows: $ER = (Cl_H/Q_H)$

MDCK-MDR1 Permeability Assay

The permeability and efflux of JNJ-64413739 were measured using Madin-Darby Canine Kidney Cells (MDCK) cells transfected with the P-glycoprotein (MDR1). The assay was performed at Cyprotex (Watertown, MA, USA).

MDR1-MDCK cells obtained from the NIH (Rockville, MD, USA) are used between passage numbers 6-30. Cells are seeded onto Millipore Multiscreen Transwell plates at 3.4×10^5 cells/cm². They are cultured for 4 days in DMEM and media is changed the day prior to the assay. On day 4 the permeability study is performed. Following culture, the monolayers are prepared by rinsing both basolateral and apical surfaces twice with buffer at pH 7.4 and 37°C. Cells are then incubated with pH 7.4 buffer in both apical and basolateral compartments for 40 min to stabilize physiological parameters.

Buffer at pH 7.4 is then removed from the apical compartment and replaced with test compound dosing solutions. The solutions are prepared by diluting 10 mM test compound in DMSO with buffer to give a final test compound concentration of 10 μ M (final DMSO concentration adjusted to 1%). The fluorescent integrity marker Lucifer yellow is also included in the dosing solution. The apical compartment inserts are then placed into 'companion' plates containing fresh buffer at pH 7.4. Analytical standards are made from dosing solutions.

For basolateral to apical (B-A) experiments the experiment is initiated by replacing buffer in the inserts then placing them in companion plates containing dosing solutions. Incubations are carried out in an atmosphere of 5% CO₂ with a relative humidity of 95% at 37°C for 60 minutes.

After the incubation period, the companion plate is removed and apical and basolateral samples diluted for analysis by LC-MS/MS. Test compound permeability is assessed in duplicate. On each plate compounds of known permeability characteristics are run as controls.

Test and control compounds are quantified by LC-MS/MS cassette analysis using a 5-point calibration with appropriate dilution of the samples. The starting concentration (C₀) is determined from the dosing solution and the experimental recovery calculated from C₀ and both apical and basolateral compartment concentrations.

The integrity of the monolayers throughout the experiment is checked by monitoring Lucifer yellow permeation using fluorimetric analysis. Lucifer yellow permeation is low if monolayers have not been damaged. If a Lucifer yellow Papp value is above QC limits in one individual test compound well, then an n=1 result is reported. If Lucifer yellow Papp values are above QC limits in both replicate wells for a test compound, the compound is re-tested. If on repeat, high Lucifer yellow permeation is observed in both

wells then toxicity or inherent fluorescence of the test compound is assumed. No further experiments are performed in this instance.

The permeability coefficient for each compound (P_{app}) is calculated from the following equation:

$$ER = \frac{P_{app(B-A)}}{P_{app(A-B)}}$$

Where dQ/dt is the rate of permeation of the drug across the cells, C_0 is the donor compartment concentration at time zero and A is the area of the cell monolayer. C_0 is obtained from analysis of the dosing solution at the start of the experiment.

In addition, an efflux ratio (ER) is calculated from mean A-B and B-A data. This is derived from:

$$ER = \frac{P_{app(B-A)}}{P_{app(A-B)}}$$

Plasma Protein Binding Assay

The plasma protein binding assay was performed at Cyprotex (Watertown, MA, USA).

Plasma containing test compound at 1 μ M is incubated at 37°C in wells that are bisected with a semi-permeable membrane. Aliquots of spiked plasma are loaded on one-half of the well and 100 mM phosphate buffer is loaded in equal volume on the other half. After a designated amount of time and after equilibrium is achieved, samples are removed and analyzed from both the buffer and plasma side to obtain free and bound concentrations.

Warfarin tested at 1 μM is used to confirm assay conditions. Literature cites warfarin as highly bound by plasma proteins. In-house, warfarin is highly bound in both rat and human, >99% and >98% respectively.

HTDialysis membranes are soaked in DI water for 15-30 minutes prior to assembling the dialysis apparatus. One mL of plasma per compound per concentration of each species is spiked with 10 μL of 100 μM compound (1 μM final concentration) and vortexed lightly for ~ 10 seconds. KPO4 buffer (150-750 μL) is added in triplicate to one side of the designated wells and the spiked plasma (150-500 μL) is added to the opposite sides. The plate is covered with adhesive sealing film and incubated on a plate agitator (100 RPM) at 37 $^{\circ}$ C for 6 hr (RED) or placed in 37 $^{\circ}$ C incubator overnight (HTDialysis).

For T = 0 samples (1 μM reference), a 50- μL aliquot (n=3) of spiked plasma is mixed with 50 μL of blank buffer and extracted with 200 μL of extraction solution (acetonitrile: methanol, 50:50) containing internal standard. Samples are vortexed for 1 minute, kept at room temperature for additional 15 minutes to release compound and to precipitate proteins and centrifuged at ~ 3200 rpm for 10 minutes. The supernatant is transferred to new tubes and stored sealed.

Post-dialysis, seal is gently removed from the plate and 50 μL of incubated plasma is added to 50 μL of blank buffer while 50 μL of incubated buffer is added to 50 μL of blank plasma. All samples are mixed with 200 μL of extraction solution (acetonitrile: methanol, 50:50, containing IS) and processed as described above.

For the LC-MS analysis, compounds are tuned and methods developed prior to incubation. Typically this process will be completed using Automaton, an automatic tuning software developed by Applied Biosystems, that selects the optimal mass transition in the MRM (Multiple Reaction Monitoring) mode on a Sciex 4000. A general LC condition is as follows:

Column: Phenomenex Synergi Hydro RP, 4 μ m, 2.0x50mm or Agilent Zorbax SB-Phenyl, 5 μ m, 2.1x50mm, flow rate: 0.8 ml/min, solvents: 0.1% formic acid in water or acetonitrile, (buffer A, B, respectively), time: 4 min. Gradient: 0.1 – 1.3 min 2%B 1.3 – 2.4 min 90% B 2.4 – 2.5 min 2% B 2.5 – 4.0 min 2% B, injection amount: 10 μ L

Samples are immediately analyzed following extracting.

Total compound concentration is determined as P'/P_0 , where P' and P_0 are the peak ratios in post dialysis and T0 plasma samples, respectively. Free compound concentration is calculated as B'/P_0 , where B' is the peak ratio in post dialysis buffer samples.

$$\% \text{ unbound} = \left(\frac{\text{free concentration}}{\text{total concentration}} \right) \times 100$$

Brain Tissue Binding Assay

The brain tissue binding assay was performed at Cyprotex (Watertown, MA, USA).

1 in 10 diluted brain tissue homogenate is prepared by adding 9 mL PBS (pH=7.4) to 1 g of brain tissue. Brain tissue homogenate, containing test compound at 5 μ M, is incubated at 37°C in the Rapid Equilibrium Dialysis (RED) Device. The RED device consists of a Teflon 48-well base plate which contains disposable inserts. These inserts are bisected by a semi-permeable (MWCO= 8 kD) membrane, creating two chambers. Aliquots (300 μ l) of spiked 1 in 10 diluted brain tissue homogenate are loaded in to one chamber and phosphate buffered saline (PBS pH=7.4, 500 μ l) is loaded into the other. The plate is then sealed and placed in a shaking incubator at 37 °C for 5 h. After 5 h, samples are removed and analyzed

from both the buffer and brain tissue homogenate side to obtain free and bound concentrations. These concentrations are then used to calculate the percentage compound bound to brain tissue (%BTB).

Venlafaxine and fluoxetine tested at 5 μM are used to confirm assay conditions.

Test compounds are received as neat compounds and diluted to 2 mM in DMSO. The final concentration in brain tissue homogenate is 5 μM .

RED inserts are in the RED base plate. Blank 1 in 10 diluted brain tissue homogenate and 2mM stock solutions are supplied to the robot. In addition, RED device and plates are placed on the robot deck (Tecan, Freedom EVO)

The robot automatically spikes brain tissue homogenate at 5 μM (final DMSO concentration in the incubation is 1%), mixes and fills RED device with buffer and spiked homogenate. All BTB measurements are performed in triplicate. The RED device is sealed and is allowed to incubate for 5 h at 37 °C on a vortex shaker (500 rpm) in an air incubator.

Calibration curves across an appropriate concentration range and quality control (QC) samples are prepared by the robot. These are used for quantitative analysis of the homogenate and buffer samples.

After incubation, the RED device is automatically sampled with the robot by taking 25 μl homogenate and 50 μl buffer, which is transferred to a 96 well plate. After addition of matrix (25 μl homogenate or 50 μl buffer, 50 μl DMSO and 300 μl acetonitrile) the samples are ready for LC-MS/MS analysis.

Samples are analyzed by LC-MS/MS in Multiple Reaction Monitoring (MRM) mode. One LC-MRM method is used for all tuned compounds, using optimal mass transitions and MS settings found with

tuning. Absolute concentrations of test compound in buffer and homogenate samples is quantified as measured by the calibration curve.

HPLC conditions: column: Waters Xbridge C18 3.5 μ m 4.6x50mm, Flow rate: 1.2mL/min, column temperature: Room temperature, solvent A: H2O+0.1%FA+0.5% ACN, solvent B: ACN+0.1%FA, run time: 3 min, gradient profile: 0.00 min 5 %B, 1.5 min 95 %B, 1.8 min 95 %B, 1.9 min 5 %B, 3.0 min 5% B

The formula used for determining the apparent unbound fraction ($f_{u,app}$) is as follows:

$$f_{u,app} \uparrow \frac{[A]_{buffer}}{[A]_{homogenate}}$$

where $[A]_{homogenate}$ is the concentration measured in the homogenate and $[A]_{buffer}$ the concentration measured in the buffer.

Since homogenates are diluted (in this case 10 times) the $f_{u,app}$ has to be corrected for the dilution factor in order to get the real unbound fraction in brain tissue ($f_{u,brain}$). This is accomplished with the following formula:

$$f_{u,brain} \uparrow \frac{f_{u,app}}{D \times f_{u,app} - D \times f_{u,app}}$$

Where D is the dilution factor. Subsequently, the percentage compound bound to brain tissue (%BTB) is determined as follow:

$$\%BTB \uparrow (1 - f_{u,brain}) \times 100\%$$